Polyhedron 110 (2016) 131–141

Contents lists available at ScienceDirect

Polyhedron

journal homepage: www.elsevier.com/locate/poly

A series of new heteroleptic Hg(II) complexes: Synthesis, crystal structures and photophysical properties

Shaikh M. Mobin [a,b,c,*], Anoop Kumar Saini [a], Veenu Mishra [a], Archana Chaudhary [a,*]

[a] Discipline of Chemistry, Indian Institute of Technology Indore, Simrol, Khandwa Road, Indore 452020, India
[b] Discipline of Bioscience and Biomedical Engineering, Indian Institute of Technology Indore, Simrol, Khandwa Road, Indore 452020, India
[c] Discipline of Material Science and Engineering, Indian Institute of Technology Indore, Simrol, Khandwa Road, Indore 452020, India

ARTICLE INFO

Article history:
Received 18 December 2015
Accepted 24 February 2016
Available online 4 March 2016

Keywords:
Heteroleptic
Bipyridine
Mercury
Polymer
Benzoic acid

ABSTRACT

We report the synthesis of six new heteroleptic Hg(II) complexes (**1**–**6**) with general composition [Hg(II)(bpy)L_2] where bpy = 2,2′-bipyridine, L = benzoic acid (**1**), 2-amino benzoic acid (**2**), 3-amino benzoic acid (**3**), 4-amino benzoic acid (**4**), 2-hydroxy benzoic acid (**5**), 4-hydroxy benzoic acid (**6**). **1**, **2**, **4**–**6** are monomer with hexa coordinated Hg(II) center whereas **3** is a *zig–zag* 1D-polymer with hepta-coordinated Hg(II) ion. Unlike other substituted benzoic acids, the 3-amino benzoic acid shows both $-NH_2$ and –COOH groups having affinity towards Hg(II) centers. Therefore, on reaction of $HgCl_2$/$HgBr_2$ with 3-amino benzoic acid it was observed that only $-NH_2$ group coordinates to Hg(II) center and –COOH group remains uncoordinated yielding **7** and **8**. **1**–**6** have been characterized by elemental analysis, FT-IR, thermo gravimetric analysis as well as single crystal X-ray studies. Their photo-physical properties were also investigated and maximum quantum yield was observed for **3**. Polymer **3** exhibited different fluorescence spectra in different solvents with maximum emission in chloroform. The electronic communication and geometry optimization have been performed by Density Functional Theory.

1. Introduction

Mercury is a poisonous metal and its traces may be harmful to the human body so in the recent past there is rapid development in the research of mercury sensor and detection [1–3]. Mercury has the ability of forming amalgam with almost all the metals and its copper/silver/tin amalgam is used for dental filling [4]. Generally, Hg(II) compounds find potential applications in paper industry, cosmetics, preservatives, paints, thermometers, energy efficient fluorescent light bulbs and mercury batteries [5]. Recently applications such as the antimicrobial, antibacterial, and antineoplastic of some Hg(II) complexes have been found of interest for biologist and chemist [6]. DNA–Hg complex is also useful in the probing defects in DNA [7].

The d^{10} configuration of Hg(II) is accompanied by a flexible coordination environment in such a way that the geometries of its coordination complexes may vary from distorted T-shape to octahedral to regular polyhedron. The d^{10} metal ion complexes are generally labile and formation of coordination bonds between metal ion and donor atoms of the ligand is reversible, due to this, the ligand and metal centers may rearrange during polymerization process generating highly ordered networks [8]. Consequently, Hg(II) exhibits the ability of forming all kinds of architectures *viz.* 1D, 2D and 3D polymers [5,9–12]. Carboxylic acids are versatile ligands, showing different coordination modes, monodentate, chelate, and different types of bridges [13]. Complexes of Hg(II) with various aliphatic and aromatic carboxylic acids are well documented. For instance-mercury compounds containing acetic acid [14] trifluroacetic acid [15] aminomethylphosphonic acid [16] 3-hydroxypiconic acid [17] 4-pyridylthioacetic acid [18] pyridine-3-carboxylic acid [19] 2,6-pyridynedicarboxylic acid [20–21] 2-pyridinephosphonic acid [22] have been thoroughly characterized. This literature survey prompted us to carry out a systematic study on the Hg(II) complexes containing mixed ligands. The aromatic carboxylic acid bearing another acidic or basic substituents have been used to observe the role of substituent in architect formation. Herein, we report the synthesis and characterization of eight new Hg(II) complexes, with 2,2′-bipyridine and amino/hydroxy-benzoic acids, their photophysical properties and theoretical calculations.

2. Result and discussion

Heteroleptic complexes **1**–**6** are obtained by reaction of Hg$(OAc)_2$, bpy [OAc = CH_3COO, and bpy = 2, 2′-bipyridine] and varying

* Corresponding authors at: Discipline of Chemistry, Indian Institute of Technology Indore, Simrol, Khandwa Road, Indore 452020, India (S.M. Mobin, A. Chaudhary).
E-mail addresses: xray@iiti.ac.in (S.M. Mobin), archana19jpr@gmail.com (A. Chaudhary).

http://dx.doi.org/10.1016/j.poly.2016.02.037
0277-5387/

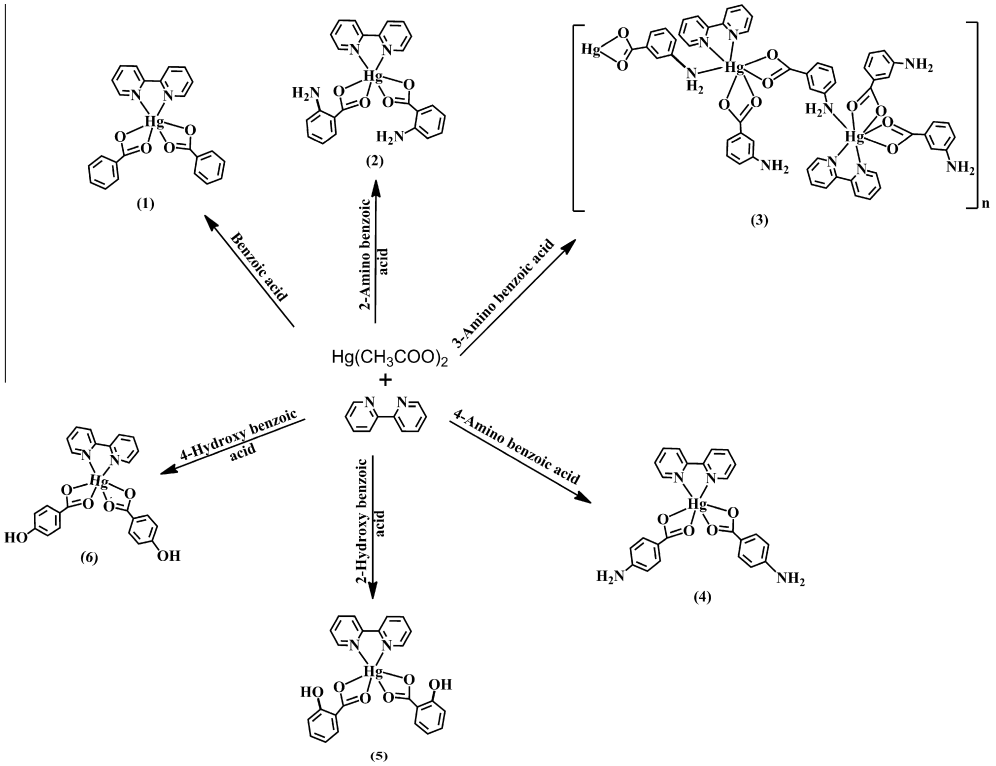

Scheme 1. Schematic representation for the synthesis of complexes **1**–**6**.

Table 1
Crystallographic parameters of complexes **1**–**8**.

Identification code	**1**	**2**	**3**	**4**	**5**	**6**	**7**	**8**
Empirical formula	$C_{24}H_{18}HgN_2O_4$	$C_{24}H_{20}HgN_4O_4$	$C_{48}H_{38}Hg_2N_8O_8$	$C_{24}H_{20}HgN_4O_5$	$C_{24}H_{18}HgN_2O_6$	$C_{24}H_{18}HgN_2O_6$	$C_{14}H_{10}Cl_2HgN_2O_4$	$C_{14}H_{10}Br_2HgN_2O_4$
Formula weight	598.99	629.04	1256.04	645.03	630.99	630.99	541.73	630.65
T (K)	150(2)	150(2)	150(2)	150(2)	150(2)	293(2)	150(2)	150(2)
Wavelength (Å)	0.71073	0.71073	0.71073	0.71073	0.71073	0.71073	0.71073	0.71073
Crystal system	monoclinic	triclinic	triclinic	monoclinic	monoclinic	monoclinic	triclinic	monoclinic
Space group	$P2_1/n$	$P\bar{1}$	$P\bar{1}$	$P2_1/n$	$P2_1/n$	$P2_1/n$	$P\bar{1}$	C_2/c
a (Å)	7.7105(8)	7.8245(9)	11.5864(3)	7.9627(2)	12.4757(14)	11.3077(13)	6.2070(8)	29.1428(9)
b (Å)	16.2556(13)	10.4766(11)	11.8687(7)	16.7257(5)	13.484(3)	16.3645(10)	7.7447(12)	4.46370(10)
c (Å)	17.0219(18)	13.5760(15)	17.3326(7)	16.9844(5)	12.781(2)	12.433(3)	16.5968(18)	12.9398(4)
α (°)	90	97.274(9)	91.704(4)	90	90	90	83.778(10)	90
β (°)	97.615(10)	91.611(9)	90.802(3)	102.626(2)	95.031(12)	106.63(2)	83.512(9)	99.134(3)
γ (°)	90	103.039(9)	109.579(4)	90	90	90	86.169(11)	90
V (Å^3)	2114.7(4)	1073.6(2)	2243.97(18)	2207.31(11)	2141.7(6)	2204.4(6)	786.85(18)	1661.93(8)
Z, D_{calc} (mg/m^3)	4, 1.881	2, 1.946	2, 1.859	4, 1.941	4, 1.957	4, 1.901	2, 2.286	4, 2.520
μ (mm^{-1})	7.312	7.209	6.898	7.018	7.232	7.026	10.140	14.089
F(000)	1152	608	1212	1248	1216	1216	508	1160
θ range	2.95–25.00	3.00–25.00	2.923–25.000	3.13–25.00	3.20–25.00	3.289–25.000	3.04–25.00	3.690–24.992
Index ranges	$-9 \leqslant h \leqslant 9$, $-18 \leqslant k \leqslant 19$, $-20 \leqslant l \leqslant 18$	$-9 \leqslant h \leqslant 9$, $-12 \leqslant k \leqslant 12$, $-16 \leqslant l \leqslant 16$	$-13 \leqslant h \leqslant 13$, $-14 \leqslant k \leqslant 10$, $-19 \leqslant l \leqslant 20$	$-9 \leqslant h \leqslant 9$, $-19 \leqslant k \leqslant 18$, $-20 \leqslant l \leqslant 20$	$-14 \leqslant h \leqslant 14$, $-15 \leqslant k \leqslant 16$, $-15 \leqslant l \leqslant 14$	$-13 \leqslant h \leqslant 8$, $-19 \leqslant k \leqslant 19$, $-14 \leqslant l \leqslant 14$	$-7 \leqslant h \leqslant 7$, $-9 \leqslant k \leqslant 8$, $-19 \leqslant l \leqslant 19$	$-33 \leqslant h \leqslant 34$, $-5 \leqslant k \leqslant 5$, $-15 \leqslant l \leqslant 15$
Reflections collected/ unique	15258/3714 [R_{int} = 0.2153]	8877/3773 [R_{int} = 0.1431]	17623/7895 [R_{int} = 0.0401]	15997/3888 [R_{int} = 0.0437]	16854/3760 [R_{int} = 0.0967]	15490/3879 [R_{int} = 0.0270]	5948/2773 [R_{int} = 0.0729]	4775/1465 [R_{int} = 0.0509]
Refinement method	Full-matrix least-squares on F^2	Full-matrix least-squares on F^2	Full-matrix least-squares on F^2	Full-matrix least-squares on F^2	Full-matrix least-squares on F^2	Full-matrix least-squares on F^2	Full-matrix least-squares on F^2	Full-matrix least-squares on F^2
Data/restraints/ parameters	3714/0/280	3773/0/306	7895/0/595	3888/0/323	3760/0/307	3879/0/298	2773/0/208	1465/0/105
Goodness-of-fit (GOF) on F^2	1.137	1.066	1.061	1.309	0.974	1.083	1.119	1.072
R_1, wR_2 [$I > 2\sigma(I)$]	R_1 = 0.0611, wR2 = 0.1569	R_1 = 0.0538, wR2 = 0.1215	R_1 = 0.0327, wR_2 = 0.0608	R_1 = 0.0471, wR_2 = 0.1075	R_1 = 0.0514, wR_2 = 0.1257	R_1 = 0.0273, wR_2 = 0.0758	R_1 = 0.0731, wR_2 = 0.1865	R_1 = 0.0457, wR_2 = 0.1237
R_1, wR_2 (all data)	R_1 = 0.0856, wR_2 = 0.1844	R_1 = 0.0839, wR_2 = 0.1587	R_1 = 0.0426, wR_2 = 0.0658	R_1 = 0.0593, wR_2 = 0.1105	R_1 = 0.0598, wR_2 = 0.1303	R_1 = 0.0352, wR_2 = 0.0773	R_1 = 0.0791, wR_2 = 0.1935	R_1 = 0.0480, wR_2 = 0.1259
CCDC No.	1415542	1415543	1415540	1415539	1415541	1415546	1415544	1415545

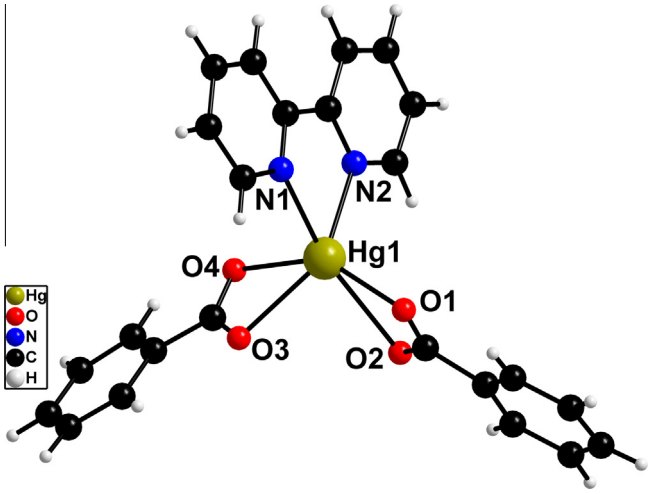

Fig. 1. Perspective view of **1**.

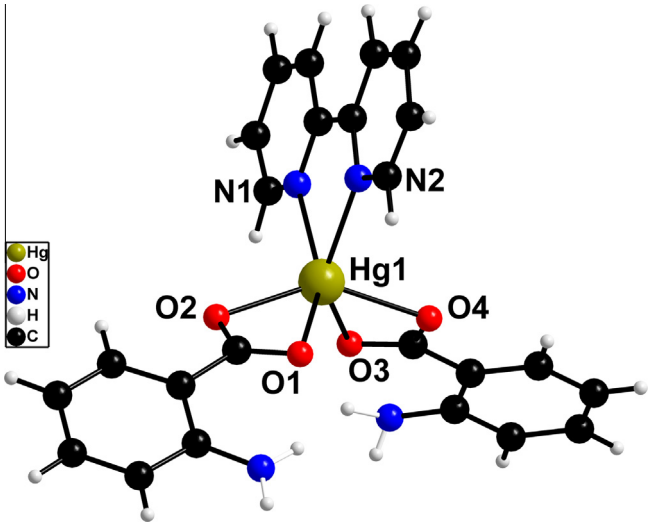

Fig. 2. Perspective view of **2**.

aromatic acids, *i.e.*, benzoic acid(BA) (**1**), 2-amino benzoic acid(2-ABA) (**2**), 3-amino benzoic acid(3-ABA) (**3**), 4-amino benzoic acid (4-ABA) (**4**), 2-hydroxy benzoic acid(2-HBA) (**5**), and 4-hydroxy benzoic acid(4-HBA) (**6**) in acetonitrile (ACN) at 298 K (Scheme 1). The progress of these reactions has been monitored by thin layer chromatography (TLC) and **1**–**6** are obtained in good yield. All these complexes are stable at room temperature with poor solubility in common organic solvents. **1**–**6** have been characterized by elemental analysis, FT-IR, and UV–Vis spectroscopy as well as by their single-crystal X-ray structures.

In **1**, **2**, **4**–**6** the carboxylic group are responsible for coordinating with Hg(II) metal center and the other substituent $-NH_2$ or –OH remains free. In contrast, the 3-ABA used in **3** shows involvement of both –COOH and $-NH_2$ groups in formation of *zig–zag* 1D polymeric chain. Further to confirm the affinity between $-NH_2$ and –COOH towards Hg(II) center, 3-ABA was reacted with $HgCl_2$/$HgBr_2$. To our surprise it was $-NH_2$ group which binds Hg (II) which result in monomers $HgX_2(3\text{-ABA})_2$ (**7**) and (**8**). Based on the Cambridge Structure Database (CSD, ConQuest Ver 1.17 updated November 2014) search, only two structures have been reported so far where 3-ABA binds to the metal {Ag(I) and Cd(II)} with amino group [23,24] leaving the carboxylic group free. Generally, 3-ABA binds to the metal either by carboxylic group or by both the donating groups.

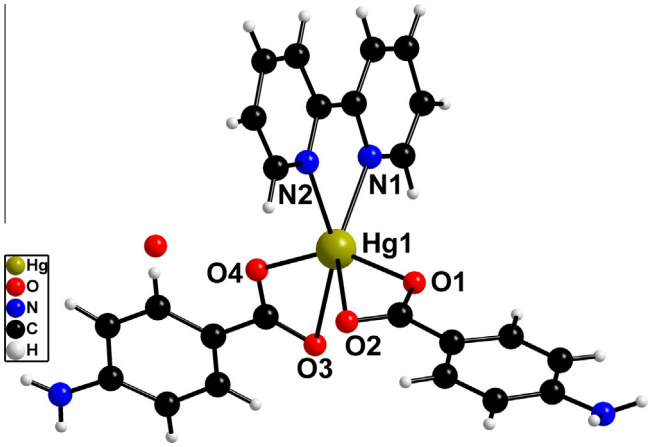

Fig. 4. Perspective view of **4**.

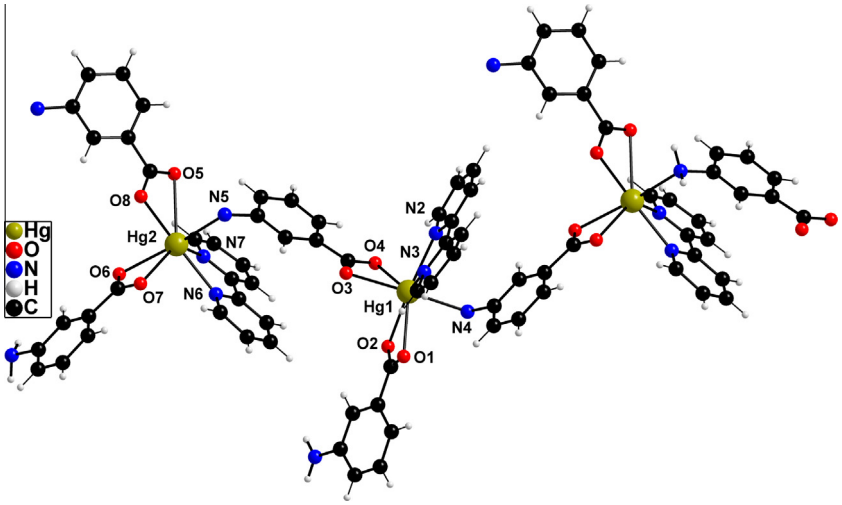

Fig. 3. Perspective view of **3**.

3. Crystal structure

1, **4**, **5** and **6** crystallize in monoclinic $P2_{1/n}$, and **2** crystallizes in triclinic $P\bar{1}$ space groups, respectively (Table 1). **1**, **2**, **4**–**6** are monomeric complexes where Hg(II) ion is present is N_2O_4 environment. The Hg(II) ion is bonded to four O atoms of carboxylate groups of two BA and two N atoms of bpy, forming distorted octahedral geometry (Figs. 1, 2 and 4–6). Hg–O bond distances are in the range of 2.149(9) Å–2.316(4) Å, whereas Hg–N bond distances ranges from 2.288(4) Å to 2.500(4) Å.

Packing diagram of **1** reveals the presence of intermolecular hydrogen bonding interaction. Intermolecular H-bonding interactions involve donor oxygen atom of BA unit and hydrogen atom of adjacent unit of another benzoic acid ring C(20)–H(20)···O(1) 2.430 Å, C(17)–H(17)···O(4) 2.445 Å, C(16)–H(16)···O(2) 2.344 Å, leading to the formation of a 1D polymeric chain (Fig. 1S) which further extends *via* C(8)–H(8)···O(2) 2.677 Å, C(9)–H(9)···O(3) 2.623 Å, forming 2D-network (Fig. 9).

Packing diagram of **2** suggests the presence of intermolecular hydrogen bonding and C–H···π interaction. C–H···π interactions involve C(1)–H(1)···π 2.492 Å, C(2)–H(2)···π 2.721 Å, yielding 1D-network (Fig. 2S) which further extends *via* C(7)–H(7)···O(4) 2.508 Å, C(9)–H(9)···O(1) 2.580 Å, and C(8)–H(8)···N(3)–C(18) 2.680 Å, generating a 2D-network (Fig. 10).

Packing diagram of **4** confirms the presence of intermolecular hydrogen bonding and C–H···π interaction. Intermolecular H-bonding interactions are present between hydrogen atom of 4-ABA H(4)N, H(23) and oxygen atom of adjacent molecule of 4-ABA O(1), O(3) C(23)–H(23)···O(3) 2.584 Å, N(4)–NH(4)···O(3) 2.274 Å, C(24)–H(24)···O(1) 2.719 Å, leading the formation of 1D-chain (Fig. 4S) which is further extended *via* C(16)–H(16)···π 2.789 Å, leading to the formation of a 2D-network (Fig. 12).

Packing diagram of **5** reveals the presence of intermolecular hydrogen bonding interaction. Intermolecular H-bonding interaction involves hydrogen H(2) of bipyridine ring and O(6) of 2-HBA unit of adjacent molecule C(2)–H(2)···O(6) 2.461 Å forming 1D-chain (Fig. 5S) which is further extended *via* C(14)–H(14)···O(4)

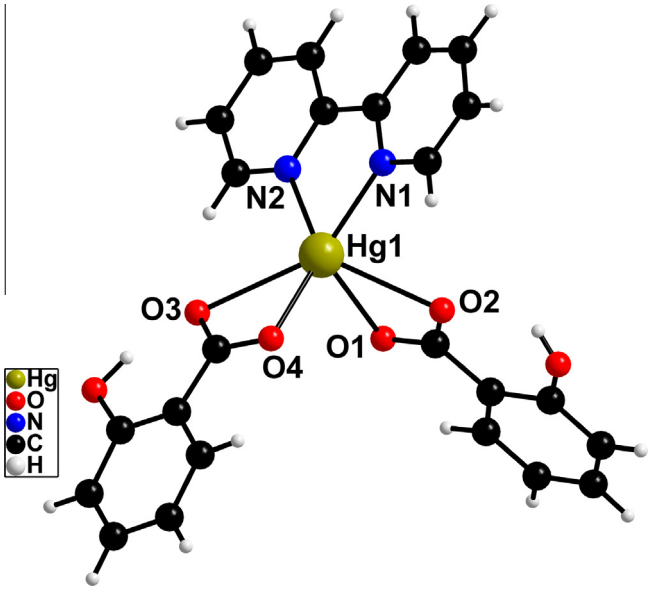

Fig. 5. Perspective view of **5**.

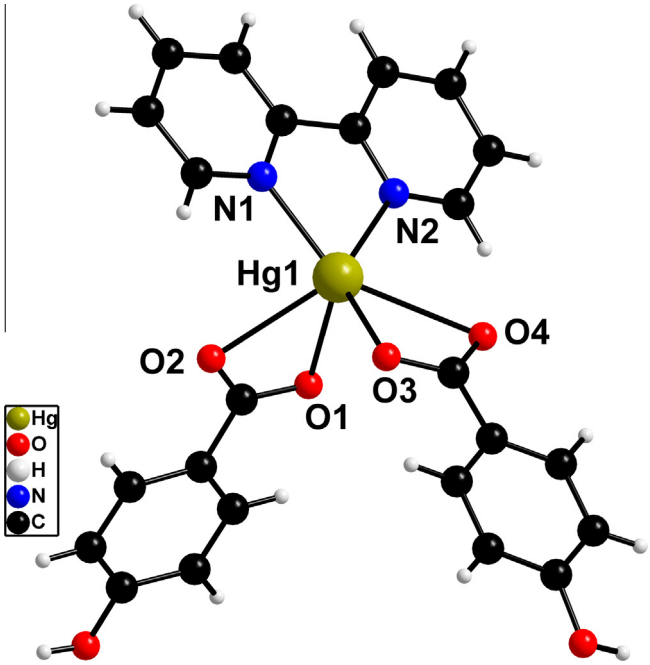

Fig. 6. Perspective view of **6**.

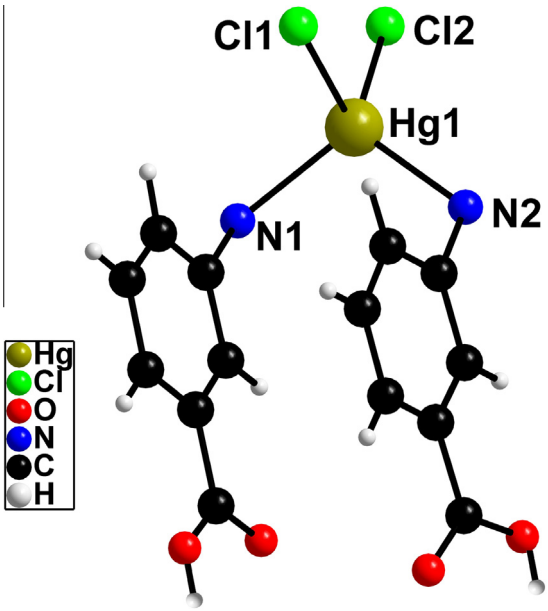

Fig. 7. Perspective view of **7**.

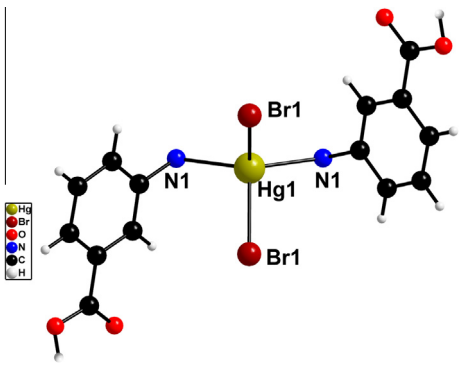

Fig. 8. Perspective view of **8**.

2.408 Å, C(15)–H(15)···O(2) 2.634 Å, leading to the formation of 2D-network (Fig. 13).

Packing diagram of **6** suggests the presence of intermolecular hydrogen bonding interaction. Intermolecular H-bonding interactions are present between oxygen and hydrogen atom of 4-HBA ring O(5), H(20) and H(16), O(3) with another 4-HBA unit of the adjacent molecule *via* C(16)–H(16)···O(5) 2.694 Å, C(20)–H(20)···O(3) 2.59 Å, leading the formation of a 1D-network (Fig. 6S) which further extends *via* C(3)–H(3)···π 3.677 Å, generating a 2D-network (Fig.14).

3 crystallizes in triclinic $P\bar{1}$ space group with crystallographic imposed inversion center (Table 1). **3** reveal formation of a *zig–zag* 1D-polymeric chain. In the 1D polymeric chain of **3**, Hg(II) is present in a distorted pentagonal bipyramidal geometry where four coordination sites are occupied by four oxygen atoms of two units of 3-ABA, two by N-atoms of bipyridine and apical position by one N-atom of 3-ABA (Fig. 3). Hg–N and Hg–O bond distances range between Hg–N 2.351(4) Å–2.500(4) Å and Hg–O 2.316 (4) Å–2.652(5) Å (Table 1). The 3-ABA molecule is coordinated to the Hg(II) ion by the carboxylate group in a bidentate manner whereas with amino group it is directly attached to the another Hg(II) ion, where 3-ABA acts as a bridging ligand between two Hg(II) ions leading to the formation of *zig–zag* 1D-polymeric chain. The two Hg(II) ions in successive monomeric unit are deviated from the mean plane by the angle of 60.31°. The dihedral angle between two 3-ABA coordinated to Hg1 and Hg2 through the carboxylate group are calculated as 87.47° and 75.04°.

Packing diagram of **3** reveals the presence of intermolecular hydrogen bonding interaction. Intermolecular H-bonding interaction involves C(39)–H(39)···O(7) 2.588 Å leading the formation of 1D-network (Fig. 3S) which further extends *via* C(31)–H(31)···π 3.682 Å leading the formation of 2D-network (Fig. 11).

Complex **7** and **8** crystallize in triclinic $P\bar{1}$ and monoclinic $C_{2/c}$ space group, respectively. In both the complexes Hg(II) atom is

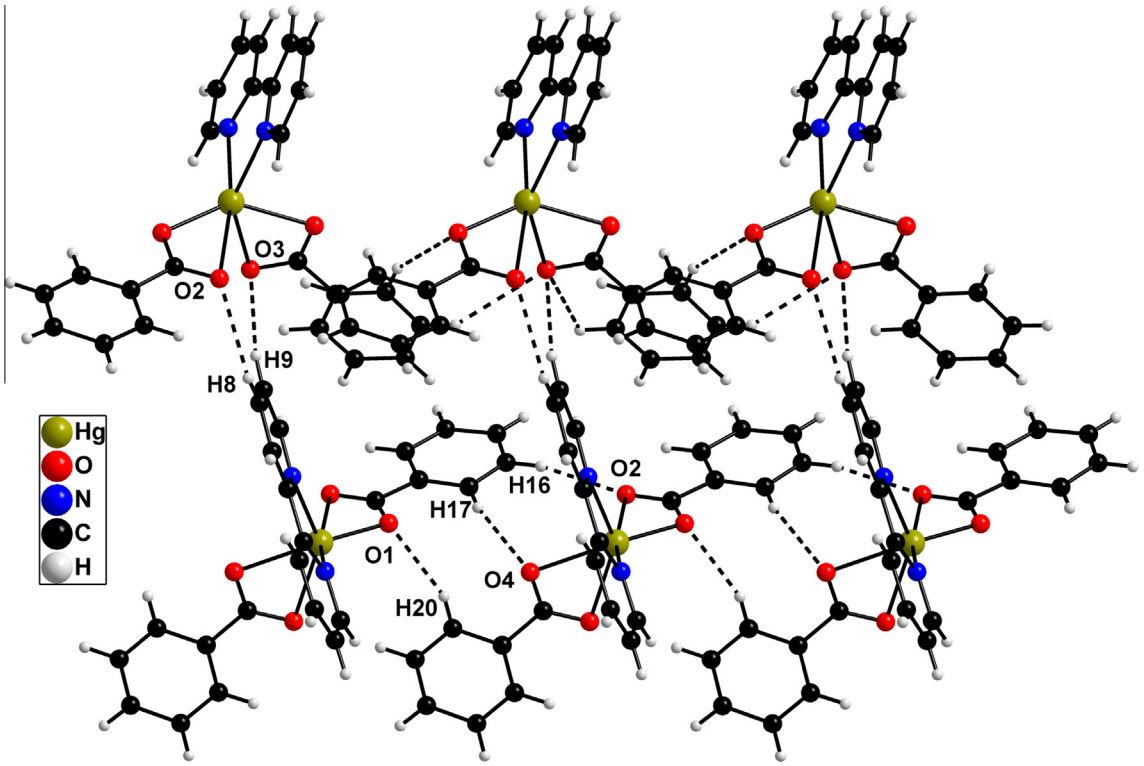

Fig. 9. Intermolecular H-bonding interactions in **1**, 2-D network.

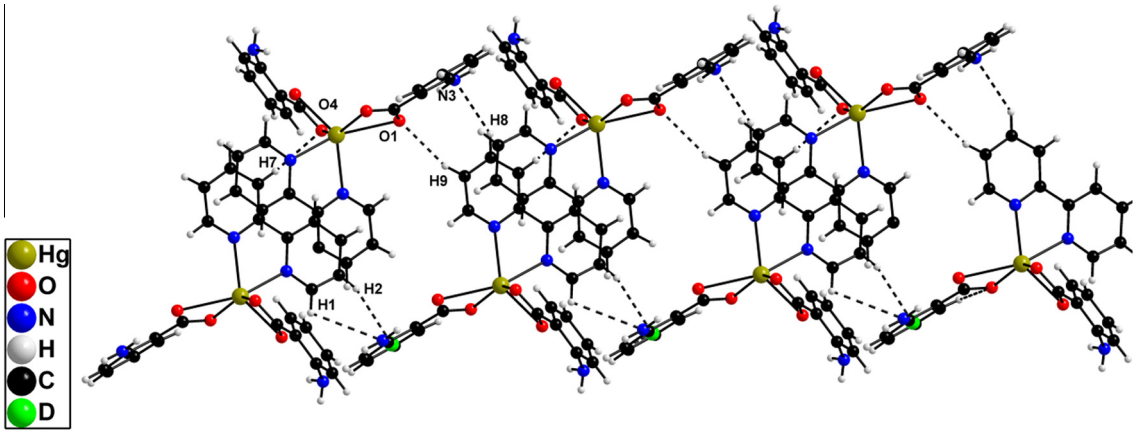

Fig. 10. Intermolecular H-bonding interactions in **2**, 2-D network (D represents centroid of the aromatic ring).

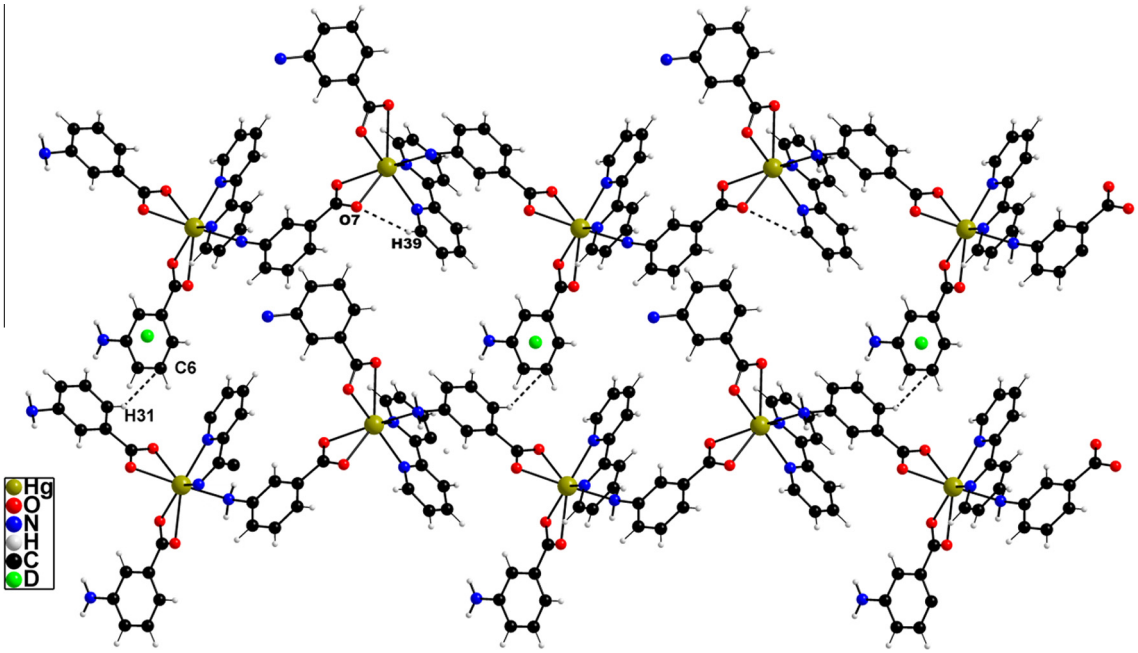

Fig. 11. Intermolecular H-bonding interactions in **3**, 2-D network (D represents centroid of the aromatic ring).

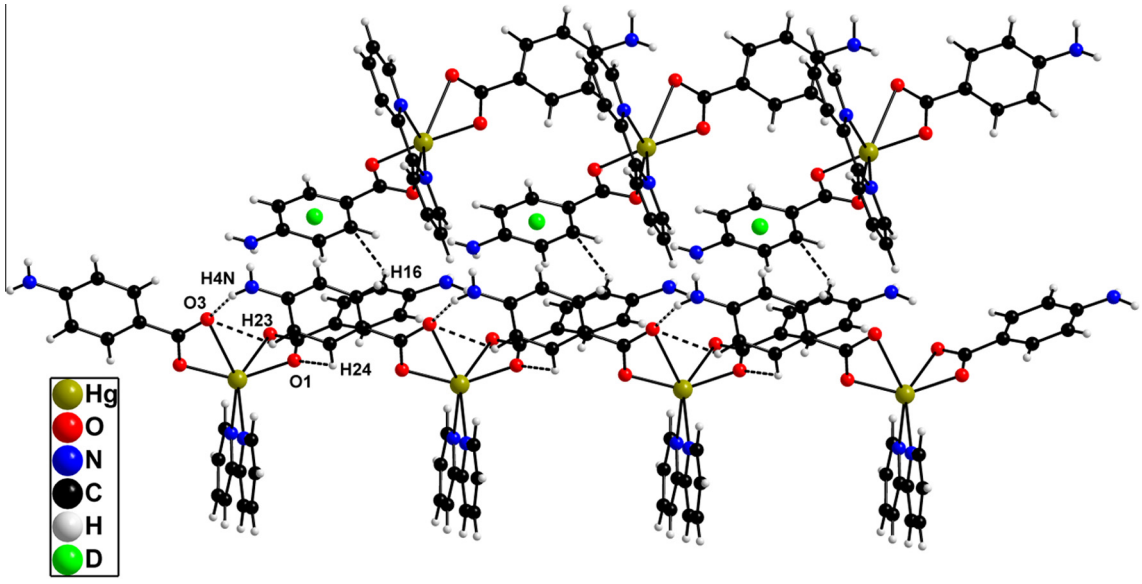

Fig. 12. Intermolecular H-bonding interactions in **4**, 2-D network (D represents centroid of the aromatic ring).

surrounded by two halide atoms and two nitrogen atoms of amino groups of two acid molecules, creating a distorted tetrahedral geometry (Figs. 7 and 8). In **7** and **8** the carboxylic group remains uncoordinated. In **7** the N(1)–Hg–N(2) bond angle was found to be 107.7° which was observed to be 131.1° in **8**. Packing diagrams of **7** and **8** reveal the presence of intermolecular hydrogen bonding interaction (Figs. 7S and 8S).

4. IR Spectra

The IR spectra of complexes **1**–**6** show strong ν(COO) absorption bands in the region 1532–1595 cm^{-1} for asymmetric stretching and in the range of 1343–1398 cm^{-1} for symmetric stretching. The observed $\Delta\nu\{\nu(COO)_{asy}-\nu(COO)_{sym}\}$ is below 200 cm^{-1} which are generally attributed to the bidentate mode of carboxylate group, while greater than 200 cm^{-1}, for the monodentate nature of the carboxylate group. A strong intensity band was observed approx. 750 cm^{-1} due to the Hg–O bond.

5. Absorption and emission spectroscopy

The electronic absorption and emission spectra of compounds **1**–**6** were recorded in chloroform at room temperature, and are displayed in Figs. 15 and 16, respectively and data are listed in Table 2. The UV–Vis spectra of **1**–**6** show three types of absorption bands. The band in the region between 300–380 nm shows weak

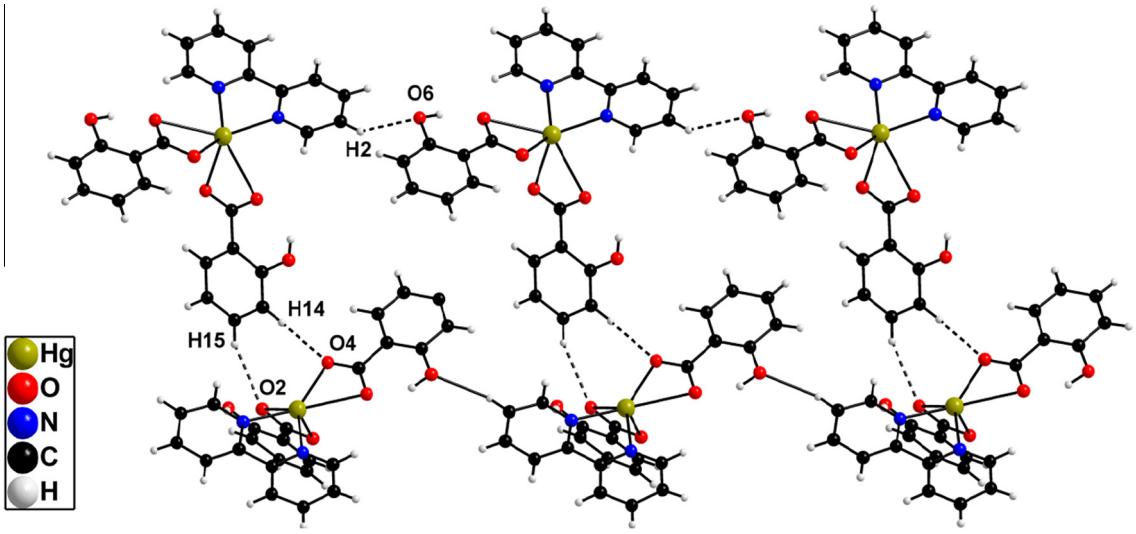

Fig. 13. Intermolecular H-bonding interactions in **5**, 2-D network.

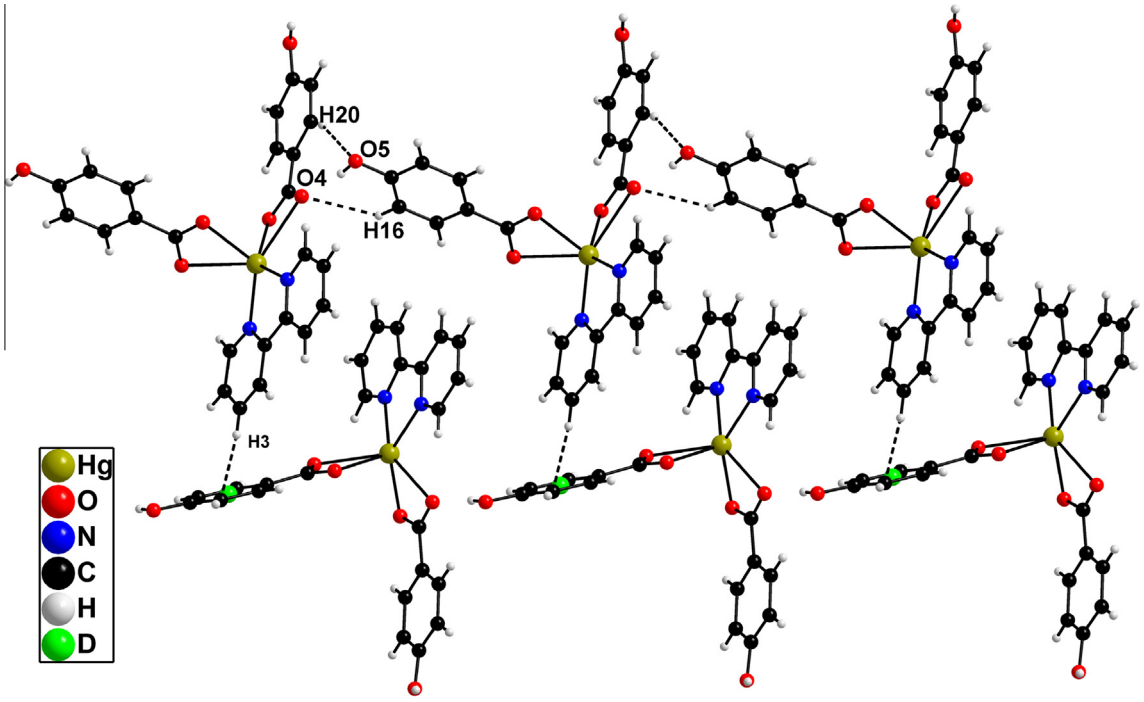

Fig. 14. Intermolecular H-bonding interactions in **6**, 2-D network (D represents centroid of the aromatic ring).

absorption peak due to $\pi \rightarrow \pi^*$ and another strong absorption band in the region of 280 nm was observed which is due to intra ligand charge transfer (ILCT) from acid unit to pyridine unit (ESI) [25]. Except **2** and **3**, other compounds show another band in the region of 235 nm which corresponds to the $\pi \rightarrow \pi^*$ transition.

When the complexes **1**–**6** in chloroform and methanol were exposed to UV lamp, they exhibited blue fluorescence but remained colorless for the other solvent (Fig. 9S). Interestingly, polymer **3** showed different emission peaks in different solvents, here maximum fluorescence was observed in chloroform and minimum in THF (Fig. 17).

The fluorescence quantum yields (Φ_F) of complexes **1**–**6** was calculated (Eq. (1) by the steady-state comparative method using Tryptophan as a standard (Φ_{st} = 0.14) [26].

$$\Phi_F = \Phi_{st} \times S_u/S_{st} \times A_{st}/A_u \times n_{Du}^2/n_{Dst}^2 \quad (1)$$

where Φ_F is the emission quantum yield of the sample, Φ_{st} is the emission quantum yield of the standard, A_{st} and A_u represent the absorbance of the standard and the sample at the excitation wavelength, respectively, while S_{st} and S_u are the integrated emission band areas of the standard and the sample, respectively, and n_{Dst} and n_{Du} are the solvent refractive index of the standard and the sample, and u and st refer to the unknown and the standard, respectively.

Compounds **1**–**6** show emission peaks on excitation at 280 nm. The maximum quantum yield (i.e., 0.089) was observed for polymer **3** and for **5** it was 0.075 whereas for **1**, **2**, **4** and **6** only ~0.007 quantum yield was calculated which is quiet less as

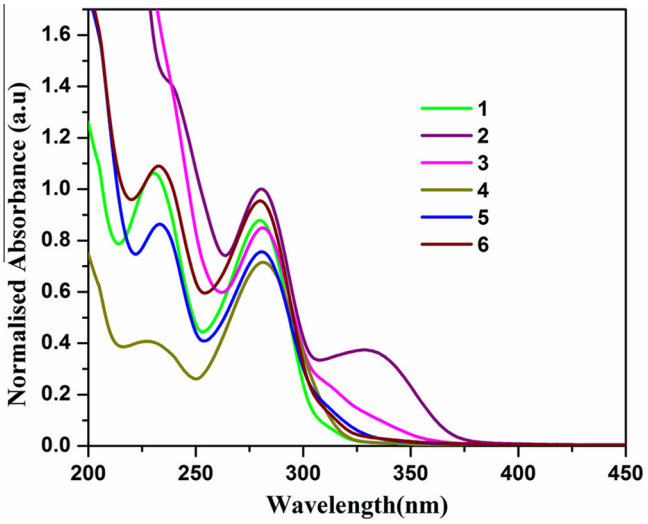

Fig. 15. Normalised electronic absorption spectra of **1**–**6** in $CHCl_3$.

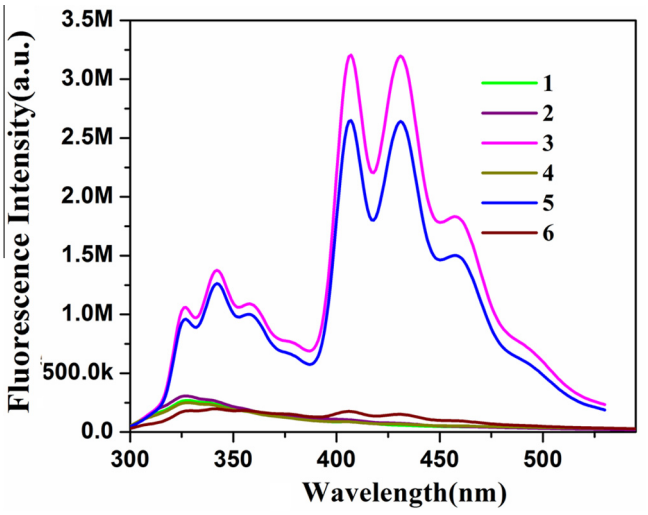

Fig. 16. Fluorescence spectra of compounds **1**–**6** in $CHCl_3$.

Table 2
Electronic properties of compounds **1**–**6**.

Compounds[a]	$\lambda_{(S0 \rightarrow S1)}$ (nm)	ε (M^{-1} cm^{-1})	λ_{ex}[b] (nm)	λ_{em}[c] (nm)	Φ[C]
1	230	31000	–	–	–
	280	26000	280	326	0.007
2	281	29000	281	325	0.008
	332	11000	–	–	–
3	281	25000	281	325, 342, 406, 431, 458	0.089
4	228	12000	–	–	–
	281	21000	281	326	0.007
5	232	25000	–	–	–
	280	22000	281	326, 342, 406, 431, 458	0.75
6	233	32000	–	–	–
	280	28000	280	327	0.008

[a] Recorded in $CHCl_3$.
[b] Excitation wavelength(nm),
[c] Excited at $\lambda_{S0 \rightarrow S1}$.
[C] Determined by using L-Tryptophan as standard (Φ_{st} = 0.14, water).

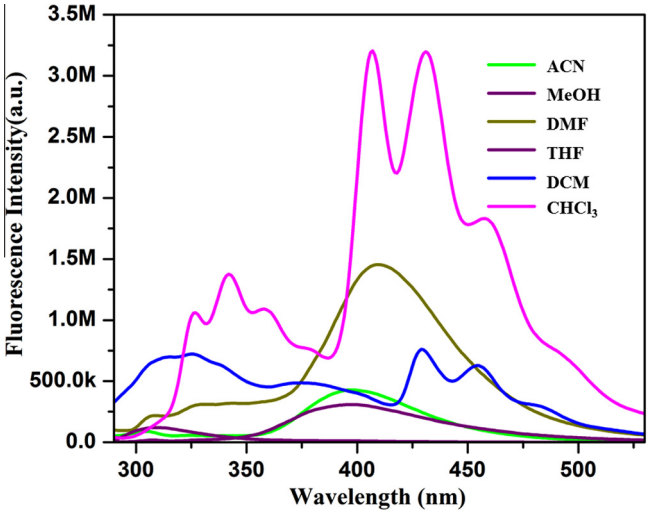

Fig. 17. Fluorescence spectra of **3** in different solvents.

compared to **3** and **5**. The higher quantum yield for 1D polymer **3** may be attributed to the higher degree of conjugation [27] whereas no appropriate reason could be found for the high quantum yield of **5**.

6. Theoretical calculations

In order to understand electronic communication, geometry optimization and energy, calculation has been done by DFT calculation. The Geometry optimization were performed using the GAUSSIAN 09 programme [28]. Two types of basis set have been used for GAUSSIAN 09 calculation. The Stuttgart-Dresden basis set (SDD) used for the mercury (Hg) atom and 6-31G basis set for Carbon (C), Hydrogen (H), Oxygen (O), Nitrogen (N) were used [29–31]. We believe such basis sets are sufficient for accurate DFT calculations. The B3LYP/6-31G, SDD functional has proven track record for the optimization of complexes and predicting the frontier orbital properties such as HOMO–LUMO energy gap [32,33]. The frontier molecular orbitals (HOMO/LUMO) of **1**, **2** and **4**–**6** are depicted in (Fig. 18). The HOMO of **1**, **2** and **4**–**6** is mainly located on nonbonding lone pairs of both acid unit and the LUMO is dispersed over π orbitals of entire 2,2′-bipyridine (bpy) units, which correlate our assumption about intra ligand charge transfer. The following energy band gap order **1** > **6** > **4** > **2** > **5** has been observed.

7. Thermogravimetric analysis

The thermal stability of the complexes **1**–**6** were carried out by thermogravimetric analysis. The thermal decomposition behavior was observed in the temperature range of 25–900 °C under the N_2 atmosphere. Complexes **4** and **5** exhibited single step decomposition while in **1**–**3** and **6**, two-step decomposition was observed (Fig. 10S).

8. Experimental

8.1. Materials

All chemicals and solvents were used as received. $(CH_3COO)_2Hg$, $HgCl_2$, $HgBr_2$, 2,2′-bipyridine, benzoic acid, 2-aminobenzoic acid, 3-aminobenzoic acid, 4-aminobenzoic acid, 2-hydroxybenzoic acid, and 4-hydroxybenzoic acid were purchased from Sigma Aldrich.

8.2. Physical measurement

Elemental analyses were performed using Thermo Scientific FLASH 2000 (formerly the Flash EA1112) elemental analyzer. Absorption spectra were recorded at ambient temperature in methanol (spectroscopy grade, Merck) solution on a Carry-100 Bio UV–Vis spectrophotometer. Fluorescence spectra were obtained on a Horiba Jobin Yvon Floromax 4P spectrophotometer. Quartz cuvettes of 10 mm optical path length received from Perkin–Elmer, USA (part No. 2345677) and Hellma, Germany (type 111-QS) were used for measuring absorption and fluorescence spectra, respectively. Fluorescence quantum yields (Φ_F) were calculated by comparing the total fluorescence intensity under the whole fluorescence spectroscopic range with that of a standard.

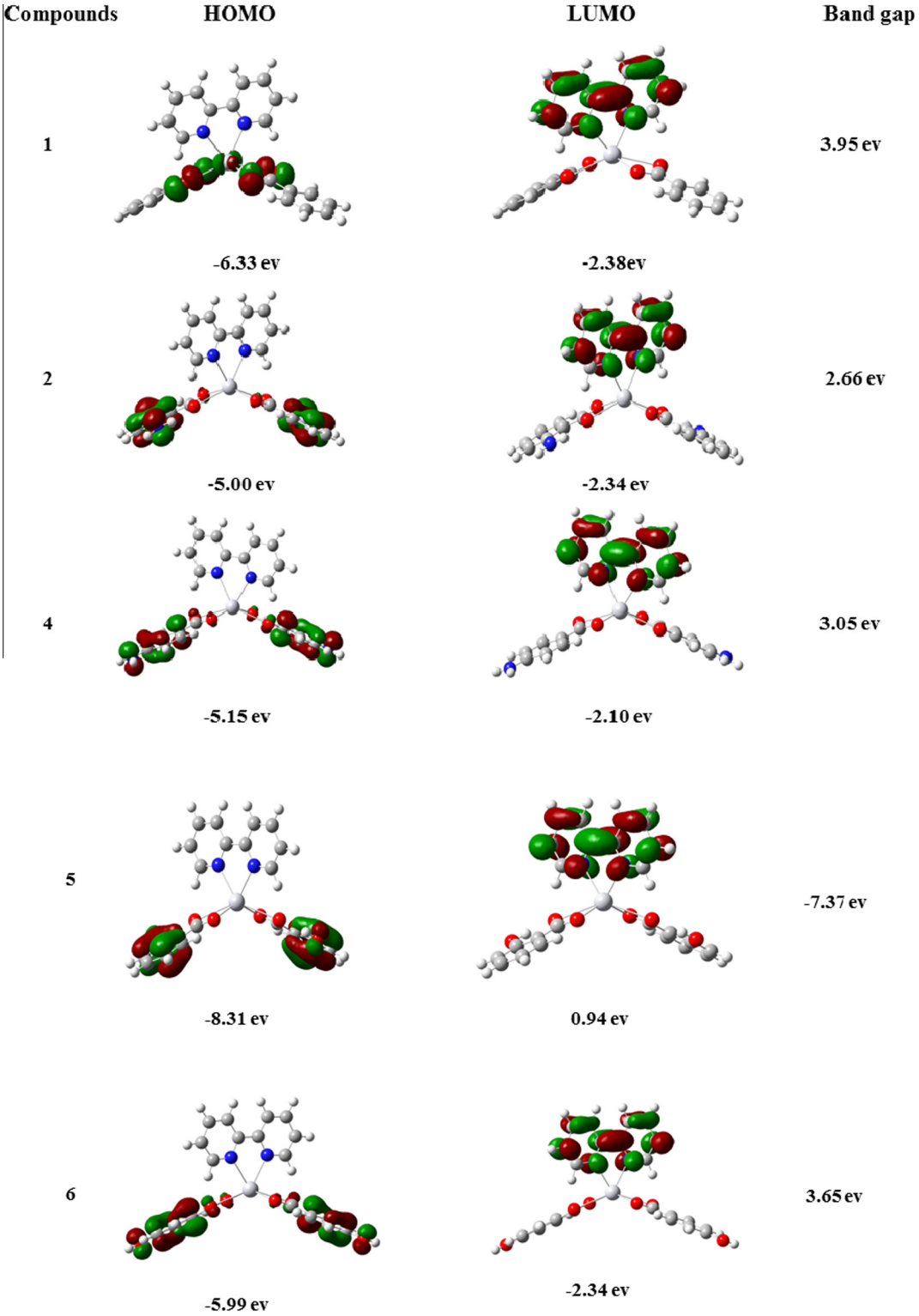

Fig. 18. HOMO and LUMO of complexes **1**, **2** and **4**–**6** and their band gap.

IR spectra [4000–400 cm^{-1}] were recorded with a Bio-Rad FTS 3000MX instrument on KBr pellets. Thermogravimetric analysis (TGA) was performed on a METTLER TOLEDO (TGA/DSC1) using software STAR^e system. The Density Functional Theory (DFT) calculations were carried out at the B3LYP/6-31G level in the GAUSSIAN 09 program.

Single crystal X-ray structural studies were performed on a CCD equipped Agilent Technology supernova diffractometer equipped with a low-temperature attachment.

8.3. X-ray crystallography

Data were collected at 150(2) K using graphite-monochromated Mo Kα (λ_α = 0.71073 Å) and Cu Kα (λ_α = 1.54814 Å). The strategy for the Data collection was evaluated, by using the CrysAlisPro CCD software. The data were collected by the standard phi-omega scan techniques and were scaled and reduced using CrysAlisPro RED software. The structures were solved by direct methods using SHELXS-97 and refined by full matrix least squares with SHELXL-97, refining on F^2 [34]. The positions of all the atoms were obtained by direct methods. All non-hydrogen atoms were refined anisotropically. The remaining hydrogen atoms were placed in geometrically constrained positions and refined with isotropic temperature factors, generally 1.2 × U_{eq} of their parent atoms. All the H-bonding interactions, mean plane analyses, and molecular drawings were obtained using the program DIAMOND (ver 3.1d). The crystal and refinement data are summarized in Table 1 and selected bond distances and bond angles are shown in Table (1S).

8.4. Synthesis of mercury complexes

8.4.1. Synthesis of $C_{24}H_{18}O_4N_2Hg$ (**1**)

To a solution of $Hg(CH_3COO)_2$ (0.318 g, 1 mmol) in acetonitrile (20 ml) benzoic acid (0.244 g, 2 mmol) and 2,2′-bipyridine (0.156 g, 1 mmol) in acetonitrile (10 ml) were added. The mixture was stirred at room temperature for overnight resulting in the formation of colorless precipitate and then mixture was filtered. Filtrate was kept as such for crystallization at room temperature, after 10–15 days needle shaped crystals formed. *Anal.* Calc. for **1** (C_{24} $H_{18}O_4N_2Hg$): C, 48.12; H, 3.03; N, 4.68. Found: C, 47.80; H, 3.30; N, 4.98). IR (KBr cm^{-1}) ν(COO) = 1595 $cm^{-1}_{(asy)}$, 1398 $cm^{-1}_{(sym)}$, 731$_{(Hg-O)}$; UV–Vis (MeOH, λ_{max} (nm (ε M^{-1} cm^{-1}))): 230 (31 000), 280 (26 000).

Complexes **2**–**6** were prepared by a similar method. Analysis for these complexes are given below.

8.4.2. Synthesis of $C_{24}H_{20}O_4N_4Hg$ (**2**)

Anal. Calc.: C, 45.83; H, 3.20; N, 8.91. Found: C, 46.06; H, 3.15; N, 8.84; IR (KBr cm^{-1}) ν(COO) = 1532 $cm^{-1}_{(asy)}$, 1391 $cm^{-1}_{(sym)}$, 758$_{(Hg-O)}$; UV–Vis (MeOH, λ_{max} (nm (ε M^{-1} cm^{-1}))): 332 (11 000), 281 (29 000).

8.4.3. Synthesis of $C_{48}H_{38}O_8N_8Hg_2$ (**3**)

Anal. Calc.: C, 41.42; H, 2.91; N, 7.90. Found: C, 41.88; H, 3.14; N, 8.24; IR (KBr cm^{-1}) ν(COO) = 1555 $cm^{-1}_{(asy)}$, 1388 $cm^{-1}_{(sym)}$, 763$_{(Hg-O)}$; UV–Vis (MeOH, λ_{max}(nm (ε M^{-1} cm^{-1}))): 281 (25 000).

8.4.4. Synthesis of $C_{24}H_{20}O_4N_4Hg$ (**4**)

Anal. Calc.: C, 45.83; H, 3.20; N, 8.91. Found: C, 45.03; H, 3.69; N, 8.44; IR (KBr cm^{-1}) ν(COO) = 1533 $cm^{-1}_{(asy)}$, 1343 $cm^{-1}_{(sym)}$, 721$_{(Hg-O)}$; UV–Vis (MeOH λ_{max}(nm (ε M^{-1} cm^{-1}))): 228 (12 000), 282 (21 000).

8.4.5. Synthesis of $C_{24}H_{18}O_6N_2Hg$ (**5**)

Anal. Calc.: C, 45.68; H, 2.88; N, 4.44. Found: C, 46.02; H, 3.35; N, 4.92; IR (KBr cm^{-1}) ν(COO) = 1578 $cm^{-1}_{(asy)}$, 1391 $cm^{-1}_{(sym)}$, 762$_{(Hg-O)}$; UV–Vis (MeOH, λ_{max} (nm (ε M^{-1} cm^{-1}))): 232 (25 000), 280 (22 000).

8.4.6. Synthesis of $C_{24}H_{18}O_6N_2Hg$ (**6**)

Anal. Calc.: C, 45.68; H, 2.88; N, 4.44. Found: C, 45.19; H, 2.91; N, 4.95; IR (KBr cm^{-1}) ν(COO) = 1570 $cm^{-1}_{(asy)}$, 1385 $cm^{-1}_{(sym)}$, 731$_{(Hg-O)}$; UV–Vis (MeOH, λ_{max} (nm (ε M^{-1} cm^{-1}): 233 (32 000), 280 (28 000).

9. Conclusion

Six new complexes of Hg(II) were synthesized and thoroughly characterized with benzoic acid and 2- or 3- or 4-amino/hydroxy benzoic acid. Reaction of $Hg(OAc)_2$ with 2- or 4-amino/hydroxy benzoic acid yielded hexa-coordinated monomers whereas with 3-amino benzoic acid hepta-coordinated Hg(II) complex is obtained generating a 1D polymer *via* $-NH_2$ group. Interestingly, 3-amino benzoic acid coordinates to the Hg(II) *via* $-NH_2$ only on reacting with $HgCl_2$ and $HgBr_2$. Polymer **3** shows different emission peaks in different solvents whereas all the other complexes are fluorescent in $CHCl_3$ and CH_3OH only.

Acknowledgements

We are grateful to CSIR, New Delhi, India for financial support and Sophisticated Instrumentation Centre (SIC), IIT Indore for instrumentation facility. A.K.S. thanks UGC, New Delhi, India and A.C. thanks CSIR, New Delhi, India for research fellowship. S.M.M. thanks CSIR, New Delhi for financial support.

Appendix A. Supplementary data

CCDC 1415542(**1**); 1415543(**2**); 1415540 (**3**); 1415539 (**4**); 1415541 (**5**); 1415546(**6**); 1415544 (**7**); 1415545 (**8**) contains the supplementary crystallographic data. These data can be obtained free of charge via http://www.ccdc.cam.ac.uk/conts/retrieving.html, or from the Cambridge Crystallographic Data Centre, 12 Union Road, Cambridge CB2 1EZ, UK; fax: (+44) 1223-336-033; or e-mail: deposit@ccdc.cam.ac.uk. Supplementary data associated with this article can be found, in the online version, at http://dx.doi.org/10.1016/j.poly.2016.02.037.

References

[1] P. Zheng, M. Li, R. Jurevic, S.K. Cushing, Y. Liu, N. Wu, Nanoscale 7 (2015). 11005-11012.
[2] À. Dago, I. González, C. Ariño, A. Martínez-Coronado, P. Higueras, J.M. Díaz-Cruz, M. Esteban, Environ. Sci. Technol. 48 (2014) 6256.
[3] S. Madhu, D. Kumar Sharma, S.K. Basu, S. Jadhav, A. Chowdhury, M. Ravikanth, Inorg. Chem. 52 (2013) 11136.
[4] T.A. DeRouen, M.D. Martin, B.G. Leroux, B.D. Townes, J.S. Woods, J. Leitão, A. Castro-Caldas, H. Luis, M. Bernardo, G. Rosenbaum, I.P. Martins, JAMA 295 (2006) 1784.
[5] A. Morsali, M.Y. Masoomi, Coord. Chem. Rev. 253 (2009) 1882.
[6] O.A. El-Gammal, G.M. Abu El-Reash, S.E. Ghazy, A.H. Radwan, J. Mol. Struct. 1020 (2012) 6.
[7] I. Kratochvílová, M. Golan, M. Vala, M. Špérová, M. Weiter, O. Páv, J. Šebera, I. Rosenberg, V. Sychrovský, Y. Tanaka, F.M. Bickelhaupt, J. Phys. Chem. B 118 (2014) 5374.
[8] G. Mahmoudi, A. Morsali, CrystEngComm 9 (2007) 1062.
[9] S.M. Mobin, V. Mishra, P. Ram, A. Birla, P. Mathur, Dalton Trans. 42 (2013) 10687.
[10] G. Mahmoudi, A. Morsali, CrystEngComm 11 (2009) 50.
[11] G. Mahmoudi, A. Morsali, M. Zeller, Inorg. Chim. Acta 362 (2009) 217.
[12] S. Caglar, Z. Heren, O. Büyükgüngör, J. Coord. Chem. 64 (2011) 2706.
[13] X.-Y. Tang, A.-X. Zheng, H. Shang, R.-X. Yuan, H.-X. Li, Z.-G. Ren, J.-P. Lang, Inorg. Chem. 50 (2011) 503.
[14] D. Grdenic, M. Sikirica, B. Korpar-Colig, Croat. Chem. Acta 62 (1989) 27.
[15] T.J. Burchell, D.J. Eisler, R.J. Puddephatt, J. Mol. Struct. 796 (2006) 47.
[16] C.R. Samanamu, E.N. Zamora, J.-L. Montchamp, A.F. Richards, J. Solid State Chem. 181 (2008) 1462.
[17] Z. Popović, D. Matković Čalogović, J. Popović, I. Vicković, M. Vinković, D. Vikić-Topić, Polyhedron 26 (2007) 1045.
[18] M. Du, C.-P. Li, Inorg. Chim. Acta 359 (2006) 1690.
[19] Z. Popović, G. Pavlović, D. Matković-Calogović, Z. Soldin, Acta Crystallogr., Sect. C 59 (2003) m165.
[20] M. Ranjbar, H. Aghabozorg, X-ray Struct. Anal. Online 20 (2004) x153.

[21] A. Moghimi, A. Shokrollahi, M. Shamsipur, H. Aghabozorg, M. Ranjbar, J. Mol. Struct. 701 (2004) 49.
[22] J.A. Fry, C.R. Samanamu, J.-L. Montchamp, A.F. Richards, Eur. J. Inorg. Chem. (2008) 463.
[23] G. Smith, B.A. Cloutt, D.E. Lynch, K.A. Byriel, C.H.L. Kennard, Inorg. Chem. 37 (1998) 3236.
[24] R. Wang, M. Hong, J. Luo, L. Han, Z.-Z. Lin, R. Cao, Acta Cryst. E59 (2003) m152.
[25] R. Luo, X. Zhou, W. Zhang, Z. Liang, J. Jiang, H. Ji, Green Chem. 16 (2014) 4179.
[26] E.P. Kirby, R.F. Steiner, J. Phys. Chem. 74 (1970) 4480.
[27] Y. Yamaguchi, Y. Matsubara, T. Ochi, T. Wakamiya, Z. Yoshida, J. Am. Chem. Soc. 130 (2008) 13867.
[28] M.J. Frisch, G.W. Trucks, H.B. Schlegel, G.E. Scuseria, M.A. Robb, J.R. Cheeseman, G. Scalmani, V. Barone, B. Mennucci, G.A. Petersson, H. Nakatsuji, M. Caricato, X. Li, H.P. Hratchian, A.F. Izmaylov, J. Bloino, G. Zheng, J.L. Sonnenberg, M. Hada, M. Ehara, K. Toyota, R. Fukuda, J.M. Ishida, T. Nakajima, Y. Honda, O. Kitao, H. Nakai, T. Vreven, J.A. Montgomery, J.J.E. Peralta, F. Ogliaro, M. Bearpark, J.J. Heyd, E. Brothers, K.N. Kudin, V.N. Staroverov, R. Kobayashi, J. Normand, K. Raghavachari, A. Rendell, J.C. Burant, S.S. Iyengar, J. Tomasi, M. Cossi, N. Rega, J.M. Millam, M. Klene, J.E. Knox, J.B. Cross, V. Bakken, C. Adamo, J. Jaramillo, R. Gomperts, R.E. Stratmann, O. Yazyev, A.J. Austin, R. Cammi, C. Pomelli, J.W. Ochterski, R.L. Martin, K. Morokuma, V.G. Voth, G. Zakrzewski, P. Salvador, J.J. Dannenberg, S. Dapprich, A.D. Daniels, Ö. Farkas, J.B. Foresman, J. V. Ortiz, J. Cioslowski, D.J. Fox, GAUSSIAN 09, Revision A.1, Gaussian Inc., Wallingford, CT, 2009.
[29] C. Lee, W. Yang, R.G. Parr, Phys. Rev. B 37 (1988) 785.
[30] A.D. Becke, J. Chem. Phys. 98 (1993) 1372.
[31] A.M. Asaduzzaman, G. Schreckenbach, Inorg. Chem. 50 (2011) 2366.
[32] H. Hou, Y. Wei, Y. Song, L. Mi, M. Tang, L. Li, Y. Fan, Angew. Chem., Int. Ed. 44 (2005) 6067.
[33] S.M. Mobin, V. Mishra, D.K. Rai, K. Dota, A.K. Dharmadhikari, J.A. Dharmadhikari, D. Mathur, P. Mathur, Dalton Trans. 44 (2015) 1933.
[34] G.M. Sheldrick, Acta Crystallogr., Sect. A. A64 (2008) 112–122. Program for Crystal Structure Solution and Refinement, University of Göettingen, Göettingen, Germany, 1997.